

Imaging of Histiocytosis in the Era of Genomic Medicine

Hyesun Park, MD
Mizuki Nishino, MD, MPH
Jason L. Hornick, MD, PhD
Eric D. Jacobsen, MD

Abbreviations: CNS = central nervous system, ECD = Erdheim-Chester disease, FDA = U.S. Food and Drug Administration, FDG = fluorine 18 fluorodeoxyglucose, H-E = hematoxylin-eosin, HLH = hemophagocytic lymphohistiocytosis, LCH = Langerhans cell histiocytosis, OR = odds ratio, RDD = Rosai-Dorfman disease

RadioGraphics 2019; 39:95–114

<https://doi.org/10.1148/rg.2019180054>

Content Codes: CH MK NR OI

From the Departments of Radiology (H.P., M.N.), Pathology (J.L.H.), and Medical Oncology (E.D.J.), Brigham and Women's Hospital and Dana-Farber Cancer Institute, 450 Brookline Ave, Boston, MA 02215. Presented as an education exhibit at the 2017 RSNA Annual Meeting. Received March 5, 2018; revision requested April 27 and received May 18; accepted May 29. For this journal-based SA-CME activity, the authors M.N. and J.L.H. have provided disclosures (see end of article); all other authors, the editor, and the reviewers have disclosed no relevant relationships. **Address correspondence to M.N.** (e-mail: Mizuki_Nishino@dfci.harvard.edu).

M.N. supported by a National Cancer Institute grant (1R01CA203636).

©RSNA, 2018

SA-CME LEARNING OBJECTIVES

After completing this journal-based SA-CME activity, participants will be able to:

- Describe the novel genomic discoveries of histiocytosis and their implications for radiologic interpretation and patient management.
- Discuss the role of imaging in diagnosing and monitoring histiocytosis in the new era of precision medicine approaches for treatment.
- Recognize the imaging characteristics of common and uncommon subtypes of histiocytosis with a focus on adult-onset cases.

See rsna.org/learning-center-rg.

Histiocytosis describes a group of diseases that have long been considered enigmatic in the history of medicine. Recently, novel genomic analyses have identified somatic oncogenic driver mutations responsible for the pathogenesis of these entities. These discoveries have led to the recharacterization of histiocytoses as neoplastic diseases and have opened a new era of precision medicine approaches for treatment. The histiocytic disorders demonstrate a variety of imaging manifestations involving multiple organ systems, and radiologists play a major role in diagnosis and monitoring. An up-to-date knowledge of the novel genomic discoveries and their implications is essential for radiologists to understand the new approaches to treating histiocytic disorders and to contribute as key members of the multidisciplinary treatment team. This article provides a cutting-edge review of the novel concepts in histiocytosis, with a focus on recent genomic discoveries and precision medicine approaches to treating the disease, and describes imaging manifestations with correlative histologic and genomic findings, with an emphasis on adult-onset cases and uncommon subtypes.

©RSNA, 2018 • radiographics.rsna.org

Introduction

Histiocytosis describes a group of disorders that result from increased proliferation of cells of macrophage or dendritic cell lineage, associated with the accumulation and infiltration of macrophages or dendritic cells in the affected tissues (1). The pathogenesis of histiocytosis has been unclear and controversial, with arguments supporting both inflammatory and neoplastic causes (2,3). However, the recent genomic discoveries of somatic oncogenic driver mutations in several subtypes of histiocytosis have defined a new concept of the entity as a neoplastic disorder. The knowledge has also led to the development of targeted molecular therapy for histiocytosis, which has opened a new era of precision medicine approaches for treating this enigmatic disease. Imaging continues to play an important role in the diagnosis and treatment monitoring of histiocytosis, and it is time for radiologists to revisit the comprehensive picture of histiocytosis under the light of novel genomic discoveries. This article presents an up-to-date review of histiocytosis, emphasizing novel genomic discoveries and precision therapy approaches, and demonstrates imaging features of the subgroups of histiocytosis, along with histologic and genomic findings, focusing on adult-onset cases and uncommon subtypes. The unmet needs in imaging of histiocytosis and future directions are also discussed.

TEACHING POINTS

- The presence of *BRAF*V600E mutation in LCH was also associated with a more severe clinical course, resistance to chemotherapy, and an increased risk of relapse.
- LCH can be classified into two groups: single-system LCH, subdivided into single site (eg, one bone lesion) and multisite (eg, multiple bone lesions), and multisystem LCH. In general, single-system LCH often involves the skin, bones, or lymph nodes, according to data from pediatric cases, while involvement of uncommon sites can be seen in sporadic cases. Single-site LCH has a high rate of spontaneous remission and a favorable prognosis.
- *BRAF*-mutant LCH is more likely to demonstrate multisystem disease with risk-organ involvement, leading to permanent and irreversible damage as seen in CNS or pituitary involvement.
- Among single-system disease in adult-onset LCH, the lungs were the most common site of involvement (51.1%) followed by bone (38.3%), in contrast to pediatric LCH, which most frequently affects the skin, bones, or lymph nodes.
- In a prospective study of 61 patients with ECD who underwent CT or MRI for abdominal findings, there was a statistically significant association between *BRAF* V600E mutation and specific imaging findings, including perinephric infiltration ($P = .003$; OR, 7.27); renal sinus and pedicle involvement ($P < .001$; OR, 14.86); sheathing or stenosis of the proximal ureters ($P < .001$; OR, 8.84); hydronephrosis ($P < .001$; OR, 8.71); adrenal gland involvement ($P < .001$; OR, 8.56); periaortic infiltration ($P = .03$; OR, 3.96); sheathing or stenosis of the renal artery ($P < .001$; OR, 10.1); and sheathing of the celiac, superior mesenteric, or inferior mesenteric arteries ($P = .04$; OR, 4.40).

Overview of Histiocytosis and Its Classification Systems

Langerhans cell histiocytosis (LCH) is the most common type of histiocytic disorder, although it is rare, with incidence rates of approximately one in 200 000 children and one in 250 000 adults (2). Historically, various terms have been used to describe LCH on the basis of the specific patterns of disease: *eosinophilic granuloma* for histiocytic infiltration for one or more lytic bone lesions; *Hand-Schüller-Christian disease* for the clinical triad of bone lesions, exophthalmos, and polyuria resulting from diabetes insipidus; or *Letterer-Siwe disease* for a fulminant course of multisystem involvement including the liver, spleen, skin, bones, and hematopoietic cells.

Gradually, the term *histiocytosis X* emerged, with the *X* as an indication of histiocyte-like cells with an incomplete understanding of the cell of origin (4). After the discovery of Birbeck granules in 1973 (5), a cytoplasmic structure associated with langerin (CD207), histiocytosis X was thought to arise from epidermal Langerhans cells, the only cells known to contain Birbeck granules at that time.

In 1987, the Writing Group of the Histiocyte Society (6) introduced a classification system of

Table 1: Conventional Classification of Histiocytosis on the Basis of Cell Type

Cell Type	Associated Diseases
Dendritic cell disorder	LCH, Erdheim-Chester disease (ECD), juvenile xanthogranuloma
Macrophage cell disorder	Rosai-Dorfman disease (RDD), primary hemophagocytic lymphohistiocytosis (HLH)
Malignant histiocytosis	Histiocytic sarcoma, interdigitating dendritic cell sarcoma

Table 2: 2016 Histiocyte Society Classification System of Histiocytic Disorders

L group	LCH, ECD
C group	Cutaneous non-LCH histiocytoses (xanthogranuloma [XG] and non-XG family)
M group	Primary malignant histiocytoses Secondary malignant histiocytoses (secondary to lymphoma, leukemia, or other histiocytoses)
R group	Familial, classic/nodal, extranodal, neoplasia-associated, and immune disease-associated RDD Other miscellaneous histiocytoses that do not belong to groups L, C, M, or H
H group	Primary HLH Secondary HLH (secondary to infection, malignancy, rheumatologic conditions, and iatrogenic conditions)

Source.—Reference 1.

histiocytosis on the basis of the putative cell of origin of the histiocytes, consisting of dendritic cell disorders, macrophage cell disorders, and malignant histiocytosis (Table 1). Dendritic cell disorders include LCH as well as ECD and juvenile xanthogranuloma. Macrophage cell disorders include RDD and HLH. Malignant histiocytosis includes diseases with much more aggressive clinical behavior such as histiocytic sarcoma and interdigitating dendritic cell sarcoma.

In 2016, an updated classification system was proposed by the Histiocyte Society (Table 2) (1). There are five different categories on the basis of histology, phenotype, molecular alterations, and clinical imaging characteristics, including the (a) Langerhans group (L group), which includes LCH and ECD; (b) cutaneous and mucocutaneous histiocytoses (C group), which consists

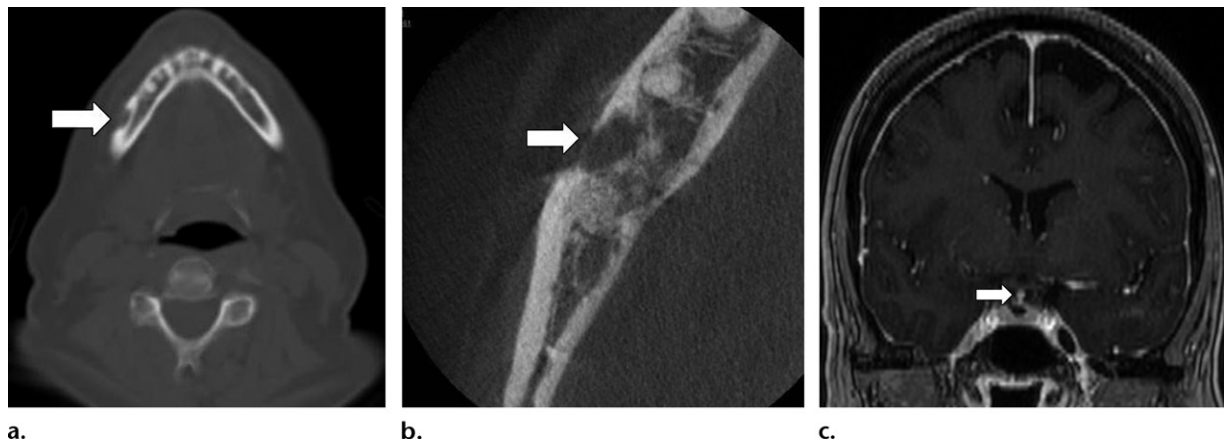


Figure 1. LCH with a *BRAF*V600E mutation in a 54-year-old woman with jaw pain. (a, b) Axial (a) and axial magnified area of interest (b) non-contrast material-enhanced CT images of the mandible show a lytic lesion (arrow) on the right. The results of a biopsy confirmed CD1a-positive and CD207-positive LCH, and the presence of *BRAF*V600E mutation was noted in the results of a genomic analysis. (c) Coronal contrast-enhanced T1-weighted MR image of the pituitary gland shows infundibular thickening (arrow), indicating pituitary involvement by LCH. The patient also demonstrated signs of diabetes insipidus.

of cutaneous non-LCH histiocytosis, with or without a major systemic component (eg, xanthogranuloma and cutaneous RDD); (c) malignant histiocytoses (M group), which includes both primary and secondary types that manifest after or simultaneously with another hematologic neoplasm; (d) RDD and other miscellaneous noncutaneous non-LCH histiocytoses (R group); and (e) HLH and macrophage activation syndrome (H group) (1).

Novel Genomic Discoveries and Clinical Applications

Over the last several decades, there has been an ongoing unanswered question among experts as to whether histiocytosis is an inflammatory disorder or a neoplastic disease. The question remained controversial because some cases of histiocytosis are self-limited with diverse inflammatory infiltrates while others involve multiple organs with a high mortality rate (2,7,8). Advances in genomic sequencing techniques and the application of this approach to histiocytosis shed light on this long-standing debate on the pathogenesis of the entity.

In 2010, with the use of the OncoMap platform designed for tumor DNA profiling, oncogenic *BRAF* V600E (a missense mutation in exon 15 with a substitution of valine with glutamic acid at amino acid 600) 21q point mutations were identified in 35 of 61 LCH samples (57%) (7) (Fig 1). Soon after, *BRAF* mutations in LCH were validated in many other studies (9–11), with a slightly lower incidence in adults compared with that in the pediatric population (38% in adults versus 47% in children) (9–12). These initial discoveries were followed rapidly by the identification of additional mutations

in the RAS/RAF pathway, including *ARAF* and *MAP2 K1* mutations (8,13,14). Moreover, *BRAF*V600E point mutations were also noted in 54% of patients with ECD, which suggested that the RAS/RAF pathway was dysregulated in a broader array of histiocytoses (15). Identification of oncogenic driver mutations indicated the neoplastic nature of the disease group and opened a possibility for novel precision therapy using RAF pathway inhibitors (16–19).

BRAF Mutation in Cancer

BRAF is a member of the RAF family of serine/threonine protein kinases. The RAS/RAF/MEK/ERK signaling pathway acts as a signal transducer between the extracellular environment and the nucleus. *BRAF* is a potent activator of MEK, leading to the activation of ERK, which then activates downstream transcription factors regulating cell proliferation, differentiation, and survival (20) (Fig 2). More than 40 different mutations have been identified in *BRAF* in human cancer. The predominant mutation in *BRAF* is in V600E. *BRAF* mutations are found in 7% of cancers, most commonly in melanoma, papillary thyroid cancer, hairy cell leukemia, and colorectal cancers (21–23).

BRAF mutations are also known to be present in subsets of patients with ovarian, breast, or lung cancers (23–26). On the basis of the knowledge of oncogenic *BRAF* mutations, precision cancer therapy using *BRAF* inhibitors has been tested in different types of cancers. Currently, vemurafenib and dabrafenib are approved for *BRAF*-mutant melanoma, and dabrafenib in combination with trametinib (MEK inhibitor) has been approved for non-small cell lung cancer with a *BRAF*V600E mutation.

BRAF Mutation in LCH

In 2010, after the identification of recurrent *BRAF* V600E mutations in LCH cases by Badalian-Very et al (7), experts in the field revisited the notion of LCH as a neoplastic rather than inflammatory proliferation and examined the implications of the *BRAF*V600E mutation on the clinical course of LCH. The presence of *BRAF*V600E mutation in LCH was also associated with a more severe clinical course, resistance to chemotherapy, and an increased risk of relapse (2,9,10). Pediatric LCH patients with *BRAF* mutation had a lower response rate to first-line chemotherapy using vinblastine and steroids than that in patients without *BRAF* mutation (78.4% vs 96.7%, respectively). More patients required second-line chemotherapy and rescue therapy in the *BRAF* mutant group than in the *BRAF* wild-type group (19.1% vs 3.5%, respectively) (10). Awareness of these accumulating data are important for radiologists so that they can be alerted to a higher risk of recurrence when interpreting imaging surveillance studies for patients with *BRAF* mutations.

Other Mutations in LCH

Although the *BRAF*V600E mutation is the most common mutation in LCH, the ERK signaling pathway is activated in pathologic histiocytes of nearly all patients with LCH, including those with wild-type *BRAF* alleles (13), indicating the presence of other oncogenic mutations in the RAS/RAF/MEK/ERK pathway in LCH. Further studies have found that mutation of mitogen-activated protein kinase 1 (*MAP2K1*), also called *MEK1*, is the second most commonly mutated gene after *BRAF*, which manifests in 25% of LCH cases (13) (Fig 2). *MAP2K1* mutations have also been reported in several other cancers, including lung and colon cancers and melanoma. Mutation in *MAP2K1* causes constitutive activation of *MAP2K1* kinase, which leads to ERK activation. In contrast to that for the *BRAF* mutation, preliminary data show that the *MAP2K1* mutations show no increased risk for initial treatment failure (27). *MAP2K1* mutations and *BRAF* mutations in LCH are usually mutually exclusive (2).

Other mutations aside from *BRAF*, *ARAF*, and *MAP2K1* mutations have been reported in LCH (2), but their clinical and therapeutic implications are unclear. Further studies are needed to comprehensively characterize the genomic background of LCH. These observations emphasize the importance of genomic characteristics of the disease to predict treatment outcome and prognosis.

BRAF and Other Mutations in ECD

Genomic discoveries in LCH led to efforts to identify oncogenic mutations in other forms of

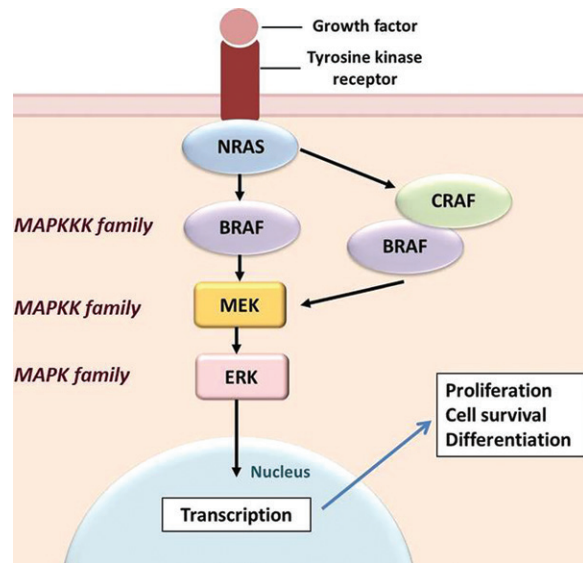


Figure 2. Illustration shows a simplified scheme of the *BRAF*/MEK/ERK signaling pathway. Extracellular signaling from transmembranous tyrosine kinase receptor acts on *NRAS*, which activates *BRAF*, leading to signaling through MEK and ERK that regulates transcription factors involved in cell proliferation, survival, and differentiation. Activating a mutation in *BRAF* V600E results in activation of the MEK/ERK signaling pathway without extracellular signaling. (Source.—References 19 and 20.)

histiocytosis. The first case of a patient with ECD harboring a *BRAF*V600E mutation was reported in 2012 (28). A subsequent study of 127 patients with histiocytosis by Haroche et al (15) demonstrated that 13 of 24 patients with ECD had a *BRAF*V600E mutation (54%). Subsequent studies have validated the presence of *BRAF* V600E mutations in 50%–60% patients with ECD. Moreover, other oncogenic mutations were detected in ECD, including a *MAP2K1* mutation in about 30% of ECD cases and *NRAS* and *KRAS* mutations in about 27% of ECD cases (2,15,29).

Precision Medicine Approaches for Treating Histiocytosis

Molecular Targeting Agents

The discovery of *BRAF* mutations has induced a potential paradigm shift in the treatment approach to histiocytosis, especially for LCH and ECD, using molecular targeting agents specifically designed to inhibit the oncogenic driver mutations. The approach is particularly relevant for adult-onset cases that have no established standard therapy and for refractory pediatric LCH, which has a poor prognosis. The association between the presence of a *BRAF* mutation and poor response to standard chemotherapy in LCH further supports the rationale for the use of *BRAF* inhibitors in treating LCH. A number of trials are ongoing to prospectively assess the efficacy of the use of *BRAF* targeting agents in

Table 3: Clinical Trials of *BRAF* Inhibitors for Histiocytosis

Trial Number	Trial Name
NCT02649972	Single-agent Cobimetinib for Adults With Histiocytic Disorders
NCT02281760	Dabrafenib and Trametinib in People With <i>BRAF</i> V600E Mutation Positive Lesions in Erdheim Chester Disease
NCT02089724	Long-term Outcome After Vemurafenib/ <i>BRAF</i> Inhibitors Interruption in Erdheim-chester Disease (LOVE)
NCT01524978	A Study of Vemurafenib in Patients With <i>BRAF</i> V600 Mutation-Positive Cancers
NCT02304809	Phase 2 Study Assessing Secured Access to Vemurafenib for Patients With Tumors Harboring <i>BRAF</i> Genomic Alterations (AcSé)

Source.—Reference 2.

Table 4: Histiocyte Society Criteria Regarding Histiocytosis Treatment Evaluation

Disease State	Disease Description	Findings	Response Category
NAD	No evidence of disease	All signs and symptoms were resolved	Better
AD	Regressive	Signs and symptoms improved, no new lesions	Better
AD	Stable	Signs and symptoms persist, no new lesions	Intermediate
AD	Mixed	Regression in one site, new lesions in another site	Intermediate
AD	Progressive	Progression and/or new lesions	Worse

Source.—Reference 34.

Note.—AD = active disease, NAD = nonactive disease.

histiocytic disorders, with cases stratified according to their *BRAF* mutation status (Table 3) (2).

The *BRAF* inhibitor vemurafenib can have dramatic efficacy in patients with ECD harboring the *BRAF*V600E mutation. Haroche et al (30,31) reported a dramatic sustained response to vemurafenib in patients with refractory ECD with *BRAF* V600E mutations. More recently, subcohort analyses of the vemurafenib basket (VE-BASKET) study demonstrate that for 22 patients with ECD and 4 patients with LCH, the confirmed overall response rate with vemurafenib was 61.5% for the overall cohort and 54.5% in patients with ECD. All evaluable patients had stable disease or better (32). These results led to the U.S. Food and Drug Administration (FDA) approval of vemurafenib use in ECD with *BRAF*V600E mutation in November 2017, a landmark achievement in the targeted therapy of histiocytosis (33).

Treatment Response Evaluations as an Area of Growing Need

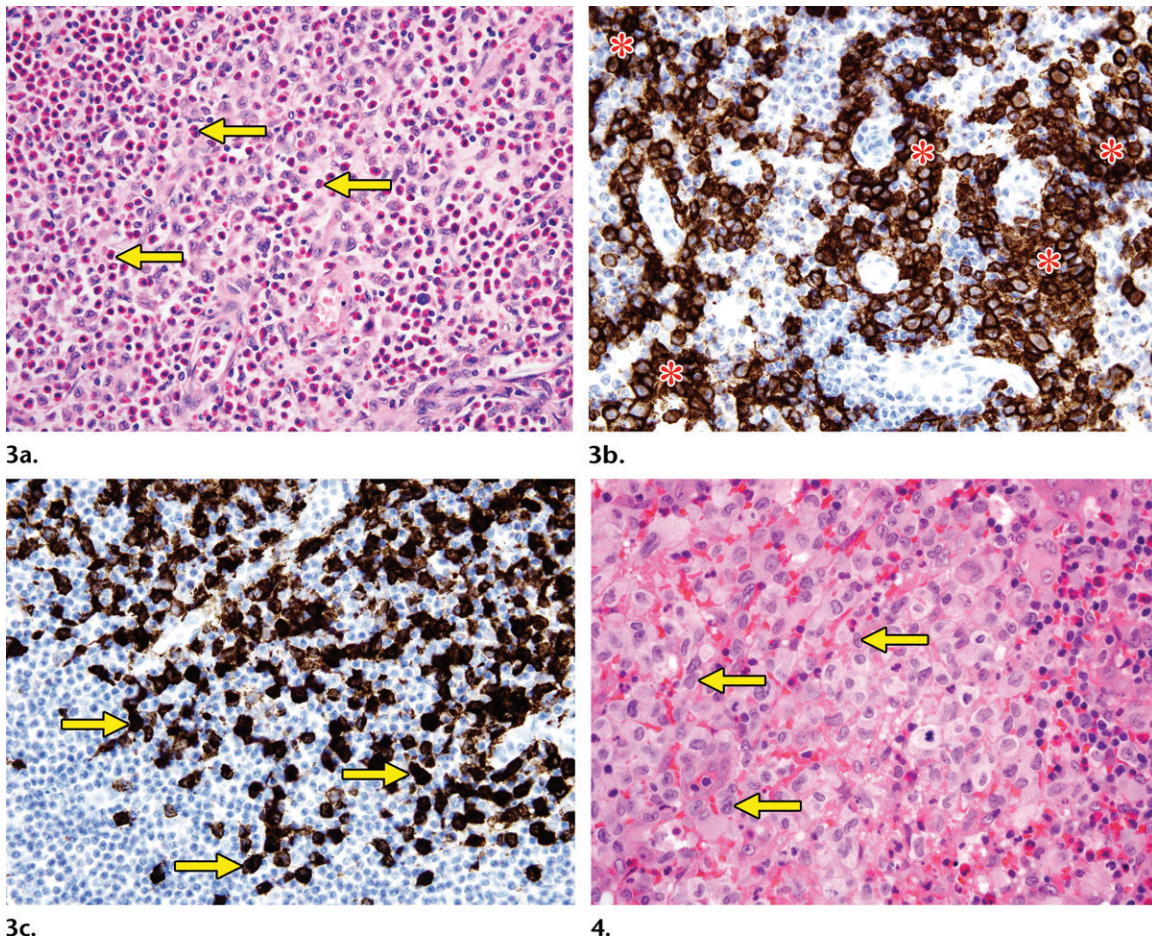
It has been well recognized that imaging plays a key role in assessing treatment response to therapy in neoplastic disorders and helps define the efficacy of novel therapeutic agents (34,35). The Histiocyte Society Evaluation and Treatment Guidelines describe criteria for response

evaluation to therapy in histiocytosis (Table 4) (36). The criteria categorize responses into three groups (better, intermediate, or worse), predominantly on the basis of qualitative assessment of signs, symptoms, and disease burden (36). Moreover, recent studies including the VE-BASKET study used the Response Evaluation Criteria in Solid Tumors (RECIST) for patients with LCH and ECD, as it is the standardized criteria for patients with advanced cancer, and the trial included patients with advanced malignancy other than LCH (32). However, histiocytosis has unique multisystem involvement with a wide spectrum of disease manifestations, including osseous lesions and interstitial lung disease, which may not be adequately evaluated by RECIST guidelines that are designed to evaluate solid metastatic lesions of advanced cancers.

Given the emerging precision medicine approaches with novel targeted agents for histiocytosis, further efforts are needed to standardize and optimize treatment response criteria specifically designed for histiocytosis to meet the new demands.

Updated Radiologic Views of Histiocytosis: LCH

In light of the recent advances in understanding the genomic basis of histiocytosis and its applications



Figures 3, 4. (3) Histologic features of LCH. (3a) High-power photomicrograph shows sheets of mononuclear cells, with abundant pale cytoplasm admixed with numerous eosinophils (arrows). (Hematoxylin-eosin [H-E] stain; original magnification, $\times 400$). (3b) High-power photomicrograph shows strong and diffuse expression of CD1a, noted as brown staining, most prominently seen in the areas marked by *. (Immunohistochemical stain; original magnification, $\times 400$). (3c) High-power photomicrograph shows strong staining for CD207, noted as dark brown staining (arrows). (Immunohistochemical stain; original magnification, $\times 400$). (4) Histologic features of LCH. High-power photomicrograph shows the characteristic cytologic features, including fine chromatin with irregular and folded nuclei (arrows). (H-E stain; original magnification, $\times 600$).

for treatment strategies, this section will present an updated radiologic view of the entity in association with genomic characteristics of the disease, with a particular focus on adult-onset cases of LCH. Uncommon subtypes of histiocytosis will be discussed in a later section.

LCH is the most common histiocytic disorder, characterized by the accumulation and proliferation of abnormal bone marrow–derived Langerhans-like cells. It occurs in one in 200 000 children, most commonly between ages 1 and 3 years. However, it can affect any age group from infancy through adulthood (2,37). Histologically, there are abundant CD1a–positive and CD207–positive histiocytes, often admixed with numerous eosinophils (Figs 3, 4).

Identification of Birbeck granules at ultrastructural examination led to the original assumption that LCH is derived from Langerhans cells in the skin and lymph nodes. However, further evidence favors that LCH originates

from bone marrow–derived myeloid dendritic cells (16,37).

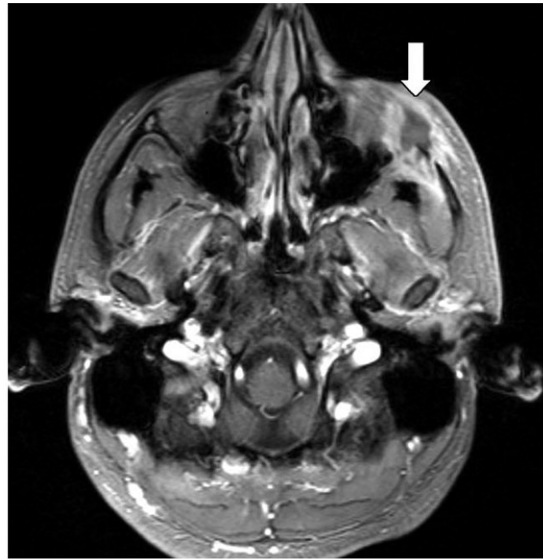
Organ System Involvement in LCH

LCH can be classified into two groups: single-system LCH, subdivided into single site (eg, one bone lesion) and multisite (eg, multiple bone lesions), and multisystem LCH (38). In general, single-system LCH often involves the skin, bones, or lymph nodes (Figs 5, 6), according to data from pediatric cases, while involvement of uncommon sites can be seen in sporadic cases (Fig 7) (39–44). Single-site LCH has a high rate of spontaneous remission and a favorable prognosis (37).

Single-site LCH often responds well to local therapy, including surgical resection and curettage, intralesional steroid injection, or radiation therapy (37). However, vertebral and craniofacial bone lesions with soft-tissue extension need special attention as these lesions may cause direct invasion or mass effect to the central nervous system



5.



6.

Figures 5, 6. (5) Single-site LCH in the bone in a 34-year-old female with a palpable lesion on the scalp. Axial CT image of the head shows a focal lytic lesion (arrow) with cortical breakthrough in the left frontal bone. The results of histologic examination confirmed LCH. (6) Single-site LCH in an 18-year-old man with facial pain and swelling. Axial contrast-enhanced T1-weighted MR image shows an irregular enhancing mass (arrow) involving the left zygomatic arch.

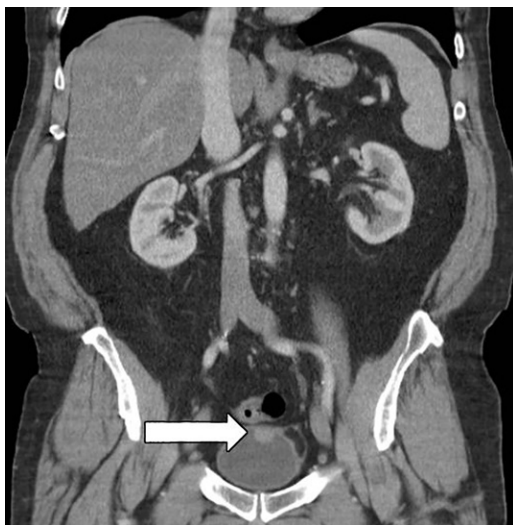


Figure 7. Single-site LCH with a bladder mass in a 59-year-old man with gross hematuria. Coronal contrast-enhanced CT image of the abdomen shows a bladder mass (arrow) arising from the upper wall of the bladder. The results of a biopsy confirmed CD1a-positive and CD207-positive LCH.

(CNS) or spinal cord, leading to neurologic symptoms or cord compression (Fig 8). Awareness of the involvement of these special sites is important when interpreting the imaging studies of patients with LCH. Single-system multisite LCH may be treated with localized treatment (eg, topical steroids for multisite skin involvement), but systemic therapy is sometimes needed.

Multisystem LCH involves two or more organs or systems. The clinical course of multisystem

LCH can be unpredictable, with a small subset of cases characterized by rapid deterioration and lethal outcome or long-term disease leading to high morbidity (37). Involvement of a risk organ, which includes the liver, spleen, and bone marrow, is an important prognosticator for multisystem LCH because it is associated with a less favorable prognosis, with mortality up to 20% on the basis of the data on pediatric cases (36) (Fig 9).

Of note, in cases of dysfunction of the liver (indicated by hepatomegaly, hypoproteinemia, and hypoalbuminemia), splenomegaly, or hematopoietic involvement (including cytopenia as an indicator of poor prognosis), risk-adapted therapy with front-line treatment intensification are needed to improve outcome (37,45). Imaging plays an important role in detecting risk-organ involvement in cases of multisystem LCH.

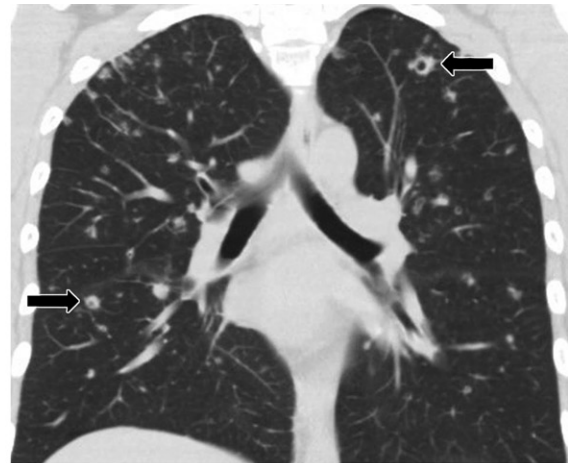
BRAF-mutant LCH is more likely to demonstrate multisystem disease with risk-organ involvement, leading to permanent and irreversible damage as seen in CNS or pituitary involvement (Fig 10) (2,10). In a French cohort study of 315 pediatric LCH cases, *BRAF* mutation was noted in 87.8% of multisystem LCH cases with risk-organ involvement, in 68.6% of multisystem LCH cases without risk-organ involvement, and in 43.9% of single-system LCH cases without risk-organ involvement (10).

Compared with that of wild-type *BRAF*, *BRAF* V600E mutation was independently associated with risk-organ involvement (odds ratio [OR], 6.35) and with skin involvement (OR,

Figure 8. CNS risk lesion in a 40-year-old woman with LCH with right supraorbital pain. Axial contrast-enhanced CT image obtained at the level of the orbits shows an expansile peripheral enhancing lesion (arrow) in the right frontal sinus, eroding the inner and outer tables, with extensive inflammatory changes in the pre-septal and periorbital tissues and extension into the epidural space, representing a CNS risk lesion. The results of a biopsy confirmed LCH positive for S-100, CD68, CD1a, CD207, and *BRAF* mutation.



a.



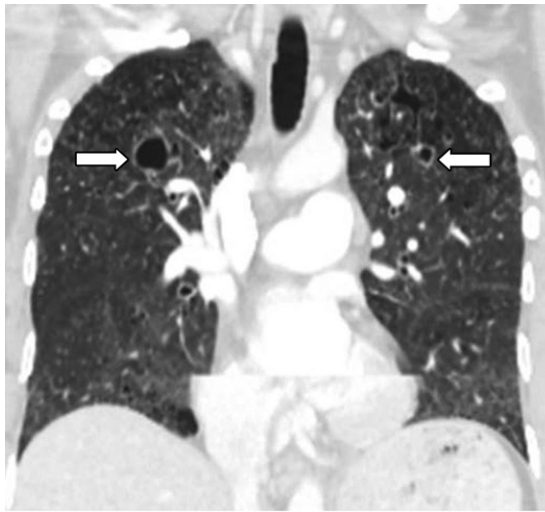
b.

Figure 9. Multisystem LCH with risk-organ involvement in a 29-year-old woman with fatigue, night sweats, and right upper quadrant pain. (a) Axial CT image of the upper abdomen shows focal liver lesions (arrow), a finding consistent with LCH with risk-organ involvement, which was confirmed at histologic examination. (b) Coronal CT image of the lungs shows nodules with irregular margins and cavitation (arrows), with centrilobular distribution and upper and middle lung predominance sparing the costophrenic angle, which are characteristic findings of pulmonary involvement of LCH. The patient also underwent lung wedge biopsy, the results of which confirmed LCH in the lung.

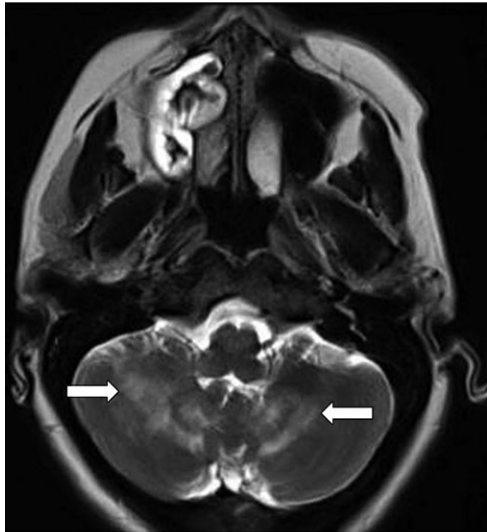
3.65) (10). With the cutting-edge knowledge of the emerging association between genomic abnormalities and the pattern of organ involvement in LCH, the radiologist may contribute to determining the precision medicine approach for treating the disease by raising the possibility of underlying *BRAF* mutation when risk-organ involvement is detected at imaging.

Patterns of disease involvement and imaging manifestations of LCH have been previously described in the radiology literature. However, most reports are based on findings in pediatric cases (46–48). Although adult-onset LCH accounts for one-third of total LCH cases (one per 560 000 adults), it remains an orphan disease, with few specialists dedicated to the entity. In addition, there have been few reports on its disease

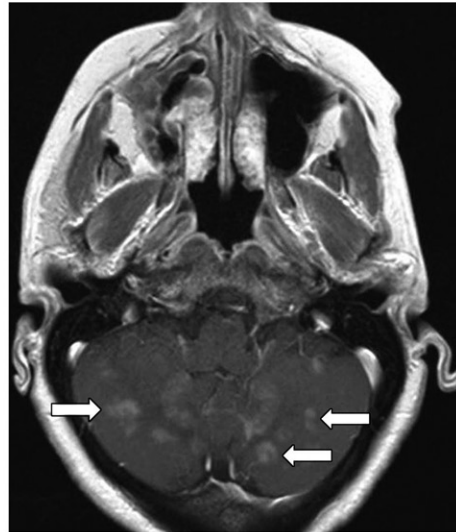
patterns at imaging (49) (Table 5). To this end, the International Histiocyte Society Registry was developed, consisting of 274 adult-onset LCH cases confirmed by the results of biopsies from 13 countries, which were analyzed to assist the clinical management of patients aged 18 years or older (49). The mean age of onset and diagnosis is 33 years, and of all patients, 31.4% had disease in a single system while 68.6% had multisystem disease. Among single-system disease in adult-onset LCH, the lungs were the most common site of involvement (51.1%) followed by bone (38.3%), in contrast to pediatric LCH, which most frequently affects the skin, bones, or lymph nodes. Multisystem disease commonly involves bone (66.0%), the lungs (61.7%), and skin (50.5%) in adults (49). Diabetes insipidus was



a.



b.



c.

Figure 10. Multisystem LCH with *BRAF* mutation with brain and lung involvement in a 40-year-old woman who was a smoker and had progressive shortness of breath, headache, ataxia, and blurry vision. (a) Coronal chest CT image shows cysts (arrows) with irregular shape, size, and nodularity, predominantly in the upper lungs, representing pulmonary LCH. The results of a biopsy confirmed LCH. (b, c) Axial T2-weighted (b) and contrast-enhanced T1-weighted (c) MR images of the brain (obtained at the time the CNS symptoms manifested) show bilateral symmetric T2 prolongation involving the cerebellum (arrows in b), with patchy areas of enhancement (arrows in c), findings indicative of neurodegenerative involvement of LCH. *BRAF* V600E mutation was confirmed by the results of a brain biopsy.

noted in 43.1% of patients with multisystem disease (Fig 11).

The 5-year survival rate from the time of diagnosis was 92.3% for the overall population, 100% for patients with single-system disease without lung involvement, 87.8% for patients with isolated lung involvement, and 91.7% for patients with multisystem disease, indicating the highest mortality for those with isolated lung involvement in adult-onset LCH, which is in contrast to that of pediatric LCH cases where risk-organ involvement is a strong prognostic indicator (49). Isolated pulmonary LCH had the strongest association with smoking history, with 77% of the group being current or

former smokers, compared to 53% in multisystem LCH with lung involvement and 30% in those without lung involvement (49).

Pulmonary LCH

Imaging manifestations of pulmonary LCH include a combination of cysts and nodules with centrilobular distribution and upper and middle lung predominance, classically sparing the costophrenic angle (50). Initial manifestation with pneumothorax is reported in 15% of patients with LCH, and pneumothorax can be recurrent (51). High-resolution CT findings are helpful in the diagnosis of LCH. In the early stage,

Table 5: Imaging Manifestations of LCH in Different Organ Systems**CNS**

Infundibular and pituitary enlargement, partially or completely empty sella, and hypothalamic involvement in the hypothalamic-pituitary axis

Symmetric T2 hyperintensity of the cerebellar white matter with “butterfly wings” appearance, T1 hyperintensity of the dentate nucleus, and T2-hyperintense areas of the pontine tegmentum in neurodegenerative LCH in the infratentorial region

Bilateral nonenhancing T2-hyperintense lesions in the cerebral white matter, and discrete symmetric T1 hyperintensity in neurodegenerative LCH in the supratentorial region

Meninges, pineal gland, choroidal lexis, or ependyma involvement in extra-axial sites

Lung

Nodules of varying sizes (1–10 mm) with indistinct margins in a peribronchovascular distribution

Pneumothorax

Round, confluent, or “bizarre” cysts, with varying wall thickness

Fibrosis with honeycombing and emphysema in upper lobes

Bone

Lytic lesions in the skull, femur, mandible, and pelvis without marginal sclerosis or periosteal reaction (“punched-out” appearance)

Vertebral plana

Accompanying soft-tissue mass

Surrounding bone marrow edema, periosteal reaction, endosteal scalloping, and soft-tissue edema at MRI

Liver

Hepatomegaly and periportal edema in the early stage

Liver cirrhosis and sclerosing cholangitis in the late stage

nodules of varying sizes with indistinct margins (1–10 mm), mainly in a peribronchovascular distribution, are visualized. Some nodules may demonstrate cavitation.

In the later stage, round, confluent, or bizarre cysts are commonly seen, and the thickness of the cyst walls varies from hairline thin to several millimeters. The size of the cysts varies and they often are 1 cm or less. However, they can be 2–3 cm or larger (Fig 12). In advanced disease, lung parenchyma can be replaced with fibrous tissue with honeycombing and emphysema, predominantly in the upper lobes (50,52–54).

CNS Manifestations of LCH

CNS manifestations of LCH include granulomatous lesions in the extra-axial regions (eg, pituitary gland and meninges) or in the intra-axial parenchymal regions and neurodegenerative LCH.

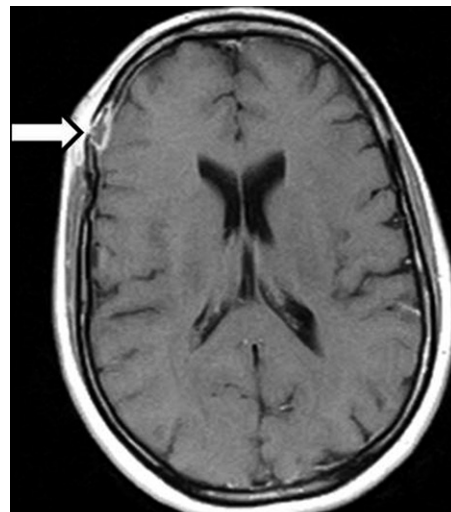
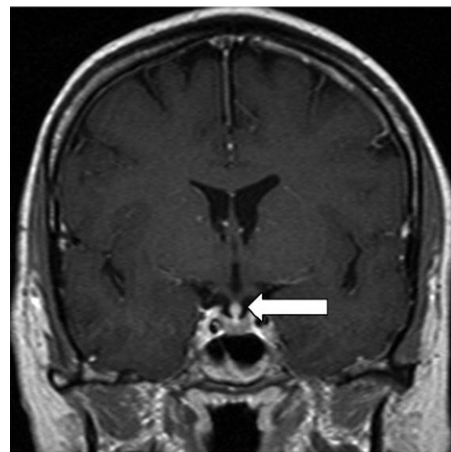
**a.****b.**

Figure 11. Multisystem LCH with bone and pituitary involvement in a 37-year-old woman with diabetes insipidus who presented with right temporal headache. **(a)** Axial contrast-enhanced T1-weighted MR image of the brain shows a right frontal bone lesion (arrow) with peripheral enhancement. **(b)** Coronal contrast-enhanced T1-weighted MR image of the brain shows nodular enhancement and thickening of the infundibulum (arrow).

Pituitary-hypothalamic involvement of LCH is the most common form, reported in 84% of patients with LCH with CNS involvement (55), and is more frequent in multisystem LCH. Diabetes insipidus can be the first clinical sign of LCH, especially in adult patients. In a study of 17 adult patients with multisystem LCH, 14 patients (82%) had an abnormality in the hypothalamic-pituitary axis at MRI (56). Infundibular enlargement was the most common finding, seen in eight patients (47%), followed by pituitary enlargement that manifested in six patients (35%). These findings were always associated with diabetes insipidus.

Other findings included a partially or completely empty sella in four patients (24%) and



Figure 12. Pulmonary LCH in a 59-year-old woman with spontaneous pneumothorax who was a former smoker. Axial CT image of the chest shows irregular-shaped cysts with thick walls (arrows) in both upper lobes, complicated with a right pneumothorax (*). The results of a biopsy confirmed pulmonary LCH.

hypothalamic involvement in three patients (18%) (56). Less frequently, LCH can involve the meninges, pineal gland, choroidal plexus, or ependyma among the extra-axial regions (55). Parenchymal involvement was reported in 44% of patients in one study (72 of 163 patients) and usually accompanies extra-axial lesions (55).

Neurodegenerative LCH is a rare progressive syndrome of neurodegeneration as a consequence of LCH, reported in 1%–5% of cases. One study of 13 patients with neurodegenerative LCH reported that 92% of patients demonstrated areas of abnormal signal intensity in the posterior fossa at MRI, including a symmetric T2 hyperintensity of the cerebellar white matter, T1 hyperintensity of the dentate nucleus, or T2-hyperintense areas of the pontine tegmentum. Symmetric T2 hyperintensity of the cerebellar white matter displays a “butterfly wings” appearance on coronal images (57). Supratentorial manifestations of neurodegenerative LCH include bilateral nonenhancing T2-hyperintense lesions in the cerebral white matter and a discrete symmetric T1 hyperintensity in the globus pallidus (57).

Osseous Involvement in LCH

Bone is commonly involved in LCH, and the lesions are often noted in the skull, femur, mandible, and pelvis (58). The osseous involvement is noted as lytic lesions, characteristically appearing as punched-out lesions in the skull, without marginal sclerosis or periosteal reaction. Osseous lesions may be accompanied by a soft-tissue mass for which radiologic evaluation of the extent of soft tissue and invasion to the adjacent structures is needed, especially in cases involving the temporal bones or orbital walls. Involvement of vertebral bodies may be noted as a vertebra plana (59).

Osseous involvement of LCH has aggressive features at MRI, demonstrating surrounding bone marrow edema, periosteal reaction, endosteal scalloping, and soft-tissue edema, which mimic findings of malignancy or infection (60). Although the results of a biopsy are often necessary to differentiate malignancy from LCH involvement owing to aggressive MRI features, it is important for radiologists to be aware of LCH as a differential diagnosis, which may help guide interpretation of the pathologic examination results.

The role of fluorine 18 fluorodeoxyglucose (FDG) PET in detecting osseous lesions in LCH has been studied in comparison with that of other imaging modalities, including CT, MRI, bone scintigraphy, and radiography, in 44 patients with LCH (41 children, 3 adults) (61). FDG PET images were superior in 90 of 256 (35%) lesions for detecting new sites or monitoring response to therapy on the basis of changes in FDG uptake before changes were noted at imaging with other modalities (61), indicating an important role of PET/CT in detecting and monitoring lesions in patients with LCH in the current clinical setting.

Liver and Lymph Node Involvement in LCH

LCH involvement of the liver is more frequent in multisystem LCH. The manifestation of liver involvement ranges from hepatomegaly and periportal edema, suggesting early liver injury, to cirrhosis and sclerosing cholangitis, suggesting late-stage injury. According to a retrospective study of 27 pediatric patients with LCH, 51.9% of patients had liver involvement (14 of 27 patients), and most of these had disseminated disease (62). LCH involving the lymph nodes usually occurs as a part of systemic disease involvement. The cervical node is the most common site of involvement (46,63).

Uncommon Subtypes of Histiocytosis

Erdheim-Chester Disease

ECD is one of the systemic histiocytoses that has been most recently classified into the L group of histiocytic disorders (1). The first two cases of ECD were reported by Jakob Erdheim and William Chester in 1930 (64). Histologically, ECD is characterized by the presence of lipid-laden histiocytes (foamy histiocytes) with surrounding fibrosis. ECD can be distinguished from LCH on the basis of clinical presentation, immunophenotype, and histopathologic characteristics. ECD is CD68 positive, CD163 positive, and CD1a negative, while LCH is CD1a and CD207 positive (Fig 13). ECD most commonly occurs in the middle-aged population during the 6th decade of life and is more prevalent in men than in women by a factor of 3:1 (2).

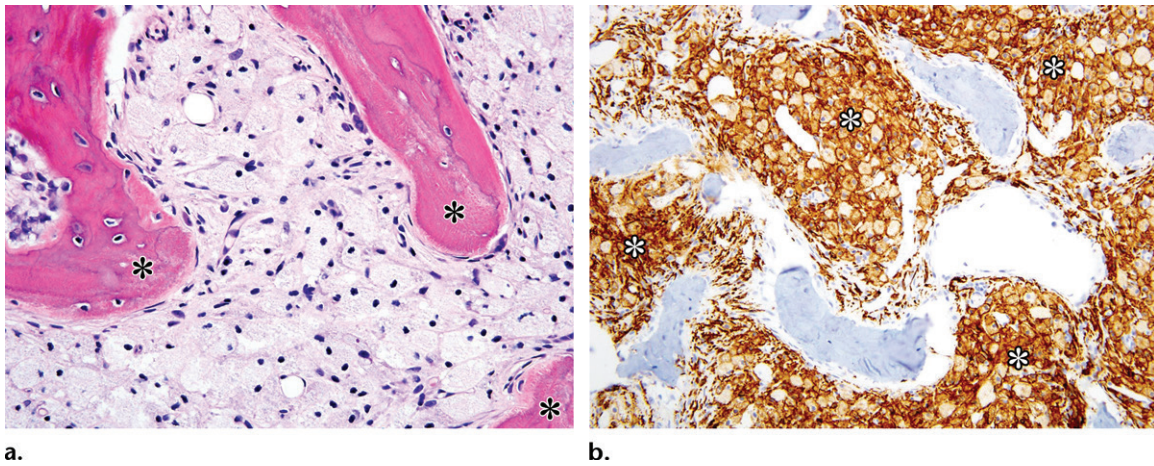


Figure 13. Histologic features of ECD. (a) High-power photomicrograph shows sheets of foamy histiocytes filling the marrow space between the bony trabecula (*). (H-E stain; original magnification, $\times 400$). (b) Medium-power photomicrograph shows strong and diffuse membranous staining for CD163, noted in most of the cells shown in the field as brown staining (*). (Immunohistochemical stain; original magnification, $\times 200$).

Radiologic manifestations of ECD are largely dependent on the site of organ system involvement (Table 6). Skeletal involvement affecting the long bones is the most common manifestation of ECD, manifesting in up to 95% of patients (65). Lower extremity involvement is more common, and bilateral symmetric cortical osteosclerosis of the diaphyseal and metaphyseal regions with epiphyseal sparing is the typical radiographic appearance and is virtually pathognomonic for ECD (66). MRI can help in the evaluation of disease extent and detection of associated osteonecrosis. Involved bone demonstrates diffuse T1-hypointense marrow signal with enhancement with sequences obtained after the administration of contrast material (postcontrast) (67). Extraosseous sites include the sinuses, large vessels, retroperitoneum, heart (particularly the pericardium and right atrium), lungs, CNS, skin, pituitary glands, and orbits.

CNS involvement occurs in approximately 50% of patients with ECD, affecting the hypothalamus and pituitary gland, brain parenchyma, orbits, or meninges (68) (Figs 14, 15). Diabetes insipidus and ataxia syndromes are common clinical manifestations of CNS disease. Hypothalamus and pituitary gland involvement manifests as infundibular enlargement or enhancement of the stalk without morphologic change and T2-weighted and/or fluid-attenuated inversion-recovery (FLAIR) hyperintensity in the hypothalamus. Infratentorial intra-axial involvement is more common than supratentorial involvement. The pons and cerebellum can be affected, showing patchy T2 and/or FLAIR hyperintensity with nodular or diffuse enhancement. Extra-axial involvement is rare but may manifest as a T1- and T2-isointense large meningeal mass with marked enhancement (68).

Table 6: Imaging Manifestations of ECD in Different Organ Systems

CNS
Infundibular enlargement, enhancement of the pituitary stalk, and T2-weighted area of hyperintensity in the hypothalamus in the hypothalamic-pituitary axis
Patchy T2-weighted area of hyperintensity with nodular or diffuse enhancement in the pons and cerebellum and a retro-orbital mass
T1- and T2-weighted isointense meningeal mass with marked enhancement
Cardiovascular
Pericardial or myocardial soft-tissue infiltration
Soft tissue around the coronary arteries
Mediastinal soft-tissue extension to the periaortic region
Lung
Smooth symmetrical interlobular septal thickening without zonal predominance
Centrilobular nodules
Focal ground-glass opacities and consolidation
Renal
Perirenal infiltration (“hairy kidney” appearance)
Bone
Bilateral symmetric cortical osteosclerosis of diaphyseal and metaphyseal lesions with epiphyseal sparing
Diffuse T1-weighted hypointense signal with contrast enhancement at MRI

Orbital involvement is rare but has a poor prognosis with progressive loss of vision. It typically manifests as exophthalmos owing to a retro-orbital mass, which is hypointense on both T1- and T2-weighted images (69). In a recent retrospective study of 32 patients with ECD who

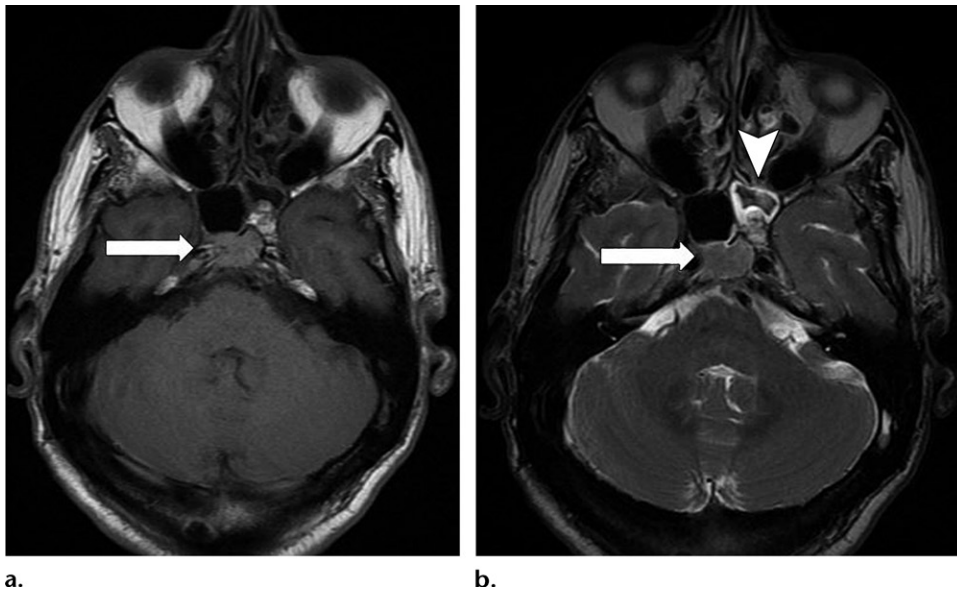


Figure 14. ECD of the clivus in a 57-year-old man with chronic headache. T1-weighted (a) and T2-weighted (b) MR images of the brain show a clival mass (arrow). Histologic examination confirmed ECD with CD68-positive and CD163-positive foamy histiocytes. The patient also has mucosal thickening in the left sphenoid sinus (arrowhead in b).

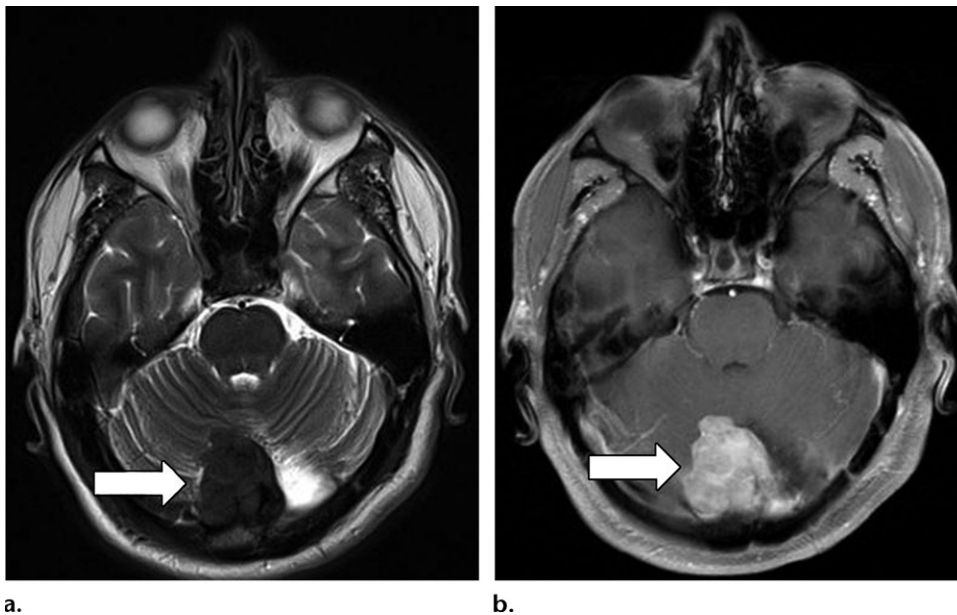
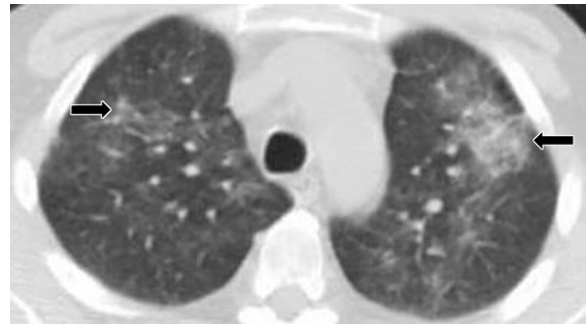


Figure 15. Cerebellar ECD in a 50-year-old man with progressively worsening headache. Axial T2-weighted (a) and contrast-enhanced T1-weighted (b) MR images of the brain show a T2-hypointense lobulated mass (arrow in a) in the cerebellum with enhancement (arrow in b). The results of a brain biopsy predominantly showed sheets of foamy histiocytes, positive for CD68 and CD163, findings associated with ECD.

underwent FDG PET/CT, the presence of *BRAF* V600E mutation was associated with FDG-avid CNS disease ($P = .0357$), higher maximum standardized uptake values ($P = .0044$), and greater mortality ($P = .0215$) (70). The presence of CNS disease had 88% specificity and 92% positive predictive value for predicting the presence of *BRAF* mutation, indicating the utility of imaging studies to guide patient management (70).

Cardiovascular involvement in ECD is often underdiagnosed; however, it occurs in 75% of patients (65,71). Pericardial involvement is the most frequent cardiac manifestation, which may result in cardiac tamponade (71,72). Soft-tissue extension around the coronary arteries is commonly accompanied by pericardial or myocardial involvement. Mediastinal involvement may demonstrate diffuse mediastinal fat or soft-tissue

Figure 16. Pulmonary involvement of ECD in a 58-year-old man with weight loss and anemia. Axial CT image of the chest shows multifocal ground-glass opacities (arrows) in both lungs. The results of a biopsy of the left upper lobe confirmed ECD with CD68-positive and CD1A-negative histiocytes infiltrating the lung.



a. **b.**
Figure 17. Perinephric ECD in a 45-year-old man with fatigue, arthralgias, and anemia. Coronal contrast-enhanced CT images of the abdomen show bilateral perinephric (arrows in a) and periaortic (arrows in b) soft tissue, characteristic findings of ECD, which were histologically confirmed to be ECD and positive for CD68 and CD163.

extension to the periaortic region (73). Lung involvement is seen in 15%–36% of cases and is noted as an interstitial lung disease, showing smooth symmetrical interlobular septal thickening that can be seen without zonal predominance (65) (Fig 16). Less commonly, centrilobular nodules or focal ground-glass opacities and consolidations can be seen (73).

Perirenal soft tissue with a “hairy kidney” appearance can be commonly seen in cases of retroperitoneal involvement, often associated with perivascular infiltration of the abdominal aorta (65) (Fig 17). Renal and vascular structures are the most commonly affected abdominal organs, and perirenal infiltration is the most prevalent finding, noted in 67% of patients at CT and MRI (74). Recent studies have investigated the association between the imaging findings and the presence of *BRAF*V600E mutation. In a prospective study of 61 patients with ECD who underwent CT or MRI for abdominal findings, there was a statistically significant association between *BRAF*V600E mutation and specific imaging findings, including perinephric infiltration ($P = .003$; OR, 7.27); renal sinus and pedicle involvement ($P < .001$; OR, 14.86); sheathing or stenosis of the prox-

imal ureters ($P < .001$; OR, 8.84); hydronephrosis ($P < .001$; OR, 8.71); adrenal gland involvement ($P < .001$; OR, 8.56); periaortic infiltration ($P = .03$; OR, 3.96); sheathing or stenosis of the renal artery ($P < .001$; OR, 10.1); and sheathing of the celiac, superior mesenteric, or inferior mesenteric arteries ($P = .04$; OR, 4.40) (74).

A gradient likelihood of a patient harboring *BRAF*V600E was also generated on the basis of the number of imaging findings, where none of the patients had *BRAF*V600E mutation in the absence of the imaging findings associated with the mutation, whereas the likelihood of the patient having *BRAF*V600E mutation was 81.3% when seven or eight imaging findings manifest (74).

Treatment with interferon α (IFN- α) has traditionally been the first-line therapy for ECD. However, long-term IFN- α treatment can lead to severe adverse effects, and patients with CNS and/or cardiovascular involvement may develop secondary resistance to high doses of IFN- α . Other agents such as anakinra, cladribine, tyrosine kinase inhibitors, and infliximab have been proposed as second-line treatments (29). On the basis of the high incidence of *BRAF* mutation in patients with ECD, accounting for up to 60% of cases, the *BRAF*

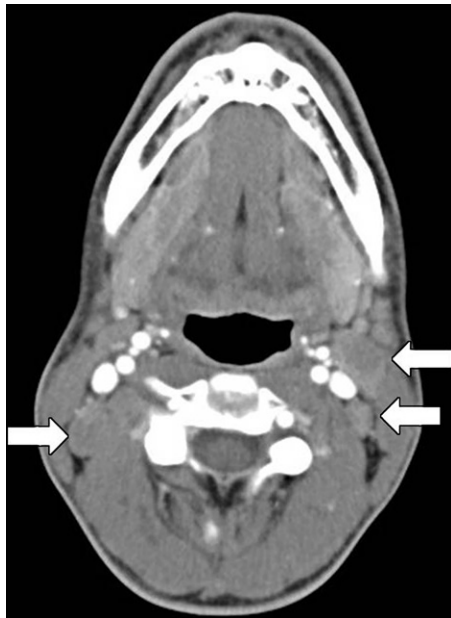


Figure 18. RDD in the cervical nodes in a 23-year-old man. Axial contrast-enhanced CT image of the neck shows bilateral cervical lymphadenopathy (arrows). The results of histologic examination confirmed prominent sinusoidal involvement by numerous large histiocytes, a finding consistent with RDD.

inhibitor vemurafenib has been tested in patients with ECD and showed significant efficacy, leading to the recent FDA approval of the agent (32).

Rosai-Dorfman Disease

RDD is a rare histiocytic disorder first described in 1965 by French pathologist Paul Destombes, who reported four children and young adults with lymphadenopathy and sinus histiocytosis (75). The disease was further characterized in 1969 as a distinct histiocytic disorder in patients with massive lymph node enlargement by two pathologists, Juan Rosai and Ronald Dorfman (Fig 18) (76).

RDD is histologically characterized by the accumulation of CD68-positive, S100-positive, CD1a-negative histiocytic cells, predominantly affecting the nodal sinuses of lymph nodes (Fig 19). Emperipolesis, the presence of intact cells (typically leukocytes within the histiocyte), is common but not required to make the diagnosis. Numerous plasma cells can be present in the lesions (2). RDD most commonly affects children but can also occur in adults and is more common in men and those of African descent.

There is no clear viral trigger, although this has long been a postulated mechanism of pathogenesis, but RDD can occur in the context of malignancies (particularly lymphoma) or rheumatologic illnesses (1,77,78). RDD may occur concurrently with Hodgkin and non-Hodgkin lymphoma or with other histiocytic disorders, and this is clas-

sified as neoplasia-associated RDD (1,79). It is often self-limited with a good prognosis. However, it can be lethal in 5%–11% of patients (2,80).

Although nodal involvement is most common, extranodal RDD is noted in 43% of cases (81) where imaging contributes to the detection and monitoring of the sites of involvement. Skin, soft tissue, the nasal cavity, bone, and retro-orbital tissue are the most common sites of extranodal disease involvement (Figs 20, 21). Osseous disease often manifests with lytic lesions (Fig 22). CNS lesions are extremely rare and may mimic meningiomas (80,82). Abdominal and pelvic organ involvement is also very uncommon. However, cases of RDD with hepatic, splenic, pancreatic, or presacral masses have been reported (83).

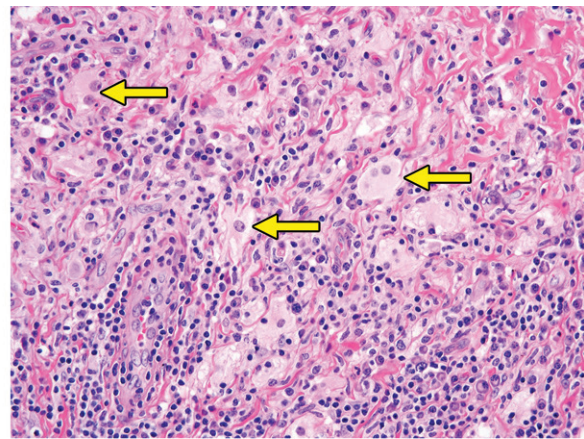
The presence of *BRAFV600E* mutations was tested in tissue samples of RDD in two studies, including a study of 47 cases by the French Histiocytosis Study Group and a study of four patients with whole exon sequencing (13,84). However, no somatic *BRAFV600E* mutations were found. A few case reports have described the presence of *KRAS* mutation in patients with RDD, including a case with a substantial response to the use of the MEK inhibitor cobimetinib (85). Although further evidence is needed to establish genomic characteristics of the disease, these reports are encouraging enough to support the initial step for precision medicine approaches for this extremely rare disease (2,84,86).

Hemophagocytic Lymphohistiocytosis

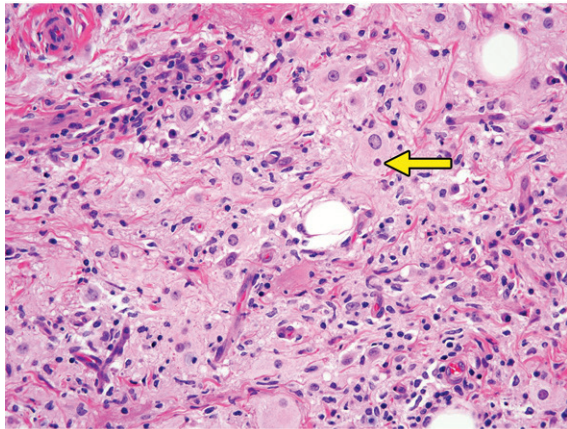
HLH is a rare disorder of intense immune activation leading to hemophagocytosis within the marrow, uncontrolled activation of T cells and macrophages, and overproduction of inflammatory cytokines (1,87,88). HLH is categorized into primary HLH (with known Mendelian inheritance), an inherited immune disorder that generally occurs in infants, and secondary HLH, which is thought to be reactive to underlying conditions such as infection, malignancies, or prolonged immunosuppression; however, distinction of the two subtypes is becoming increasingly difficult (1,88). The bone marrow, lymph nodes, spleen, liver, and CNS are the commonly involved organ systems. Clinically, patients present with fever, neurologic symptoms, and skin rash and with findings of hepatomegaly, splenomegaly, and lymphadenopathy (1,88). Treatment includes chemotherapy using etoposide or teniposide, dexamethasone, and cyclosporine, while primary HLH and selected cases of secondary HLH require bone marrow transplantation (88).

Although recognized as an often fatal disease, the survival rate is improving, and the 3-year

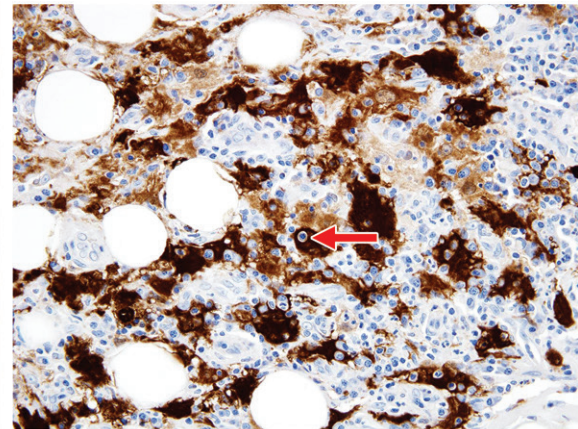
Figure 19. Histologic characteristics of RDD. (a) High-power photomicrograph shows scattered large distinctive histiocytes with voluminous pale cytoplasm and round nuclei (arrows), admixed with inflammatory cells, including lymphocytes and plasma cells. (H-E stain; original magnification, $\times 400$.) (b) High-power photomicrograph shows sheets of distinctive histiocytes, several of which contain inflammatory cells within the abundant cytoplasm. (H-E stain; original magnification, $\times 400$.) Arrow = emperipolesis. (c) High-power photomicrograph shows strong staining for S100 protein in the lesional cells. This stain also highlights emperipolesis (arrow). (Immunohistochemical stain; original magnification, $\times 400$.)



a.



b.



c.

survival is 55% in patients with primary HLH with bone marrow transplant and above 60% for those with reactive HLH (88,89). Surviving patients with HLH may experience developmental delay in the setting of radiographic or serologic evidence of CNS involvement (88).

The literature on the imaging findings of HLH is very limited given the rarity of the disease. In a retrospective study of 25 patients with HLH over an 11-year period from a single institution, nonspecific findings in the CNS, chest, and abdomen were noted that overlap with infectious, inflammatory, and neoplastic disorders (88). Alveolar-interstitial opacities with pleural effusions were common on chest radiographs, often with rapid evolution and resolution. Common abdominal findings included hepatosplenomegaly, gallbladder wall thickening, hyperechoic kidneys, and ascites. CNS findings included nonspecific periventricular white matter abnormalities, brain atrophy, and enlargement of extra-axial fluid spaces that may be progressive. In infants, some cases manifest with findings that mimic nonaccidental trauma, with intracranial hemorrhage and multiple pathologic fractures or periosteal reactions (88).

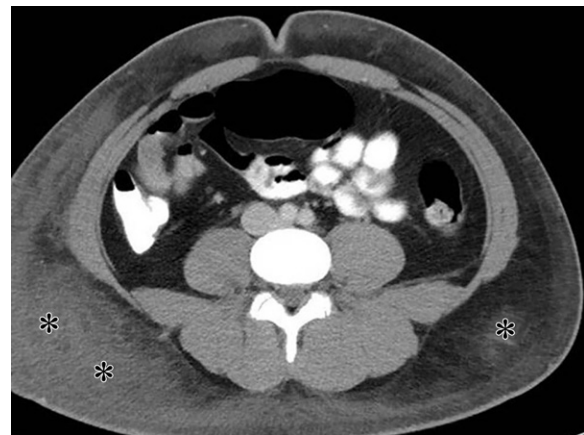


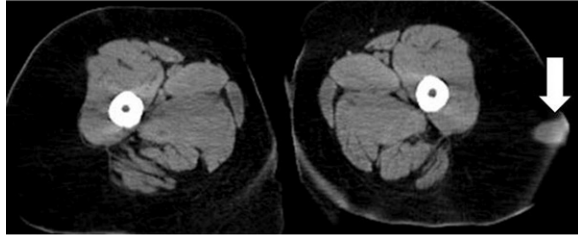
Figure 20. RDD with subcutaneous tissue involvement in a 24-year-old man with a history of lymphoma. Axial contrast-enhanced CT image of the lower abdomen shows significant stranding of the subcutaneous soft tissue (*). The results of a biopsy confirmed RDD.

Histiocytic Sarcoma

Histiocytic sarcoma is an extremely rare and aggressive subtype of histiocytosis, categorized in the group of malignant histiocytoses, or M group (1). It is histologically characterized by sheets of large epithelioid cells with marked nuclear atypia and abundant pale eosinophilic



a.



b.

Figure 21. RDD in a 64-year-old woman with a growing lung nodule and a subcutaneous nodule in the left thigh at presentation. (a) Axial CT image of the chest at the lung bases shows an oval nodule (arrow) with a slightly irregular margin in the left lower lobe. (b) Axial CT image of the upper thigh shows a subcutaneous nodule (arrow). Biopsy results for the lesions in a and b confirmed S100-positive RDD.

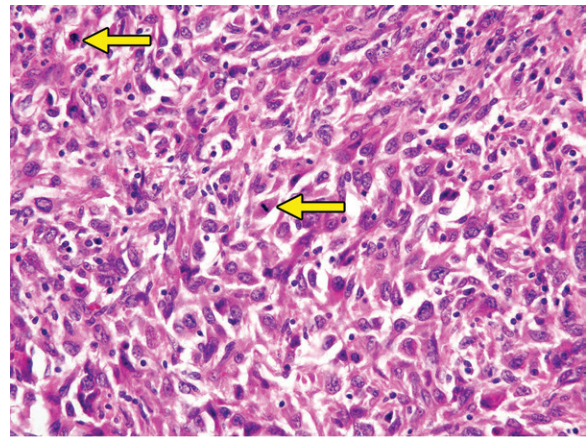


Figure 22. Osseous involvement of RDD in a 46-year-old man with back pain. Axial CT image (bone window) of the pelvis shows a lytic lesion (arrow) in the right ilium. The results of a biopsy confirmed RDD with CD68 and S100 positivity.

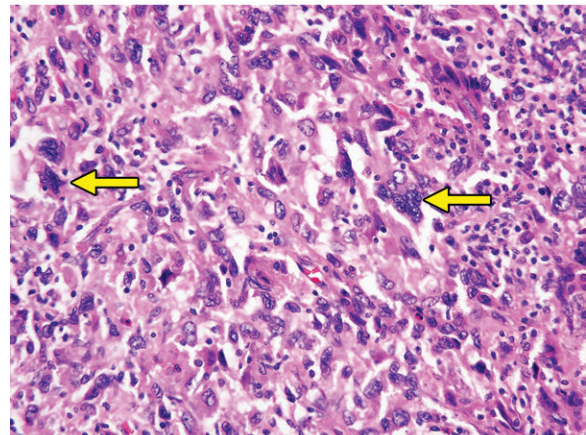
cytoplasm. Immunohistochemical markers, including CD163 and CD68, can be helpful for diagnosis (Fig 23). Primary sites of involvement are lymph nodes, skin, and the gastrointestinal tract (Fig 24). Imaging findings are nonspecific and variable depending on the site of involvement (Fig 25). Histiocytic sarcoma can occur in association with lymphoma, leukemia, or germ cell tumors.

Interdigitating Dendritic Cell Sarcoma

Interdigitating dendritic cell sarcoma is an extremely rare disease, with only 100 cases reported in the English literature (90). Clinically, it manifests as a painless mass in middle-aged men, with a male to female ratio of 3:2. Interdigitat-



a.



b.

Figure 23. Histologic and immunohistochemical features of histiocytic sarcoma. (a) High-power photomicrograph shows sheets of variably spindled epithelioid cells, with abundant pale eosinophilic cytoplasm and marked nuclear atypia. (H-E stain; original magnification, $\times 400$.) Note the scattered mitotic figures (arrows). (b) High-power photomicrograph shows markedly atypical pleomorphic cells admixed with lymphocytes. (H-E stain; original magnification, $\times 400$.) Note the multinucleated forms (arrows).

ing dendritic cell sarcoma mainly involves the lymph nodes, but extranodal involvement has been reported in one-third of cases, including in the lungs, skin, breast, bone, liver, spleen, and small intestine (90). Imaging manifestations vary depending on the disease site (Fig 26).

Conclusion

Histiocytosis demonstrates a variety of imaging manifestations involving multiple organ systems, and radiologists play a major role in its diagnosis and monitoring. Up-to-date knowledge of the novel genomic discoveries and their implications is essential for radiologists to understand the new approaches to treating histiocytosis and to contribute as key members of the multidisciplinary team. As the precision medicine approaches to treating histiocytosis further advance and become widely available, there is an

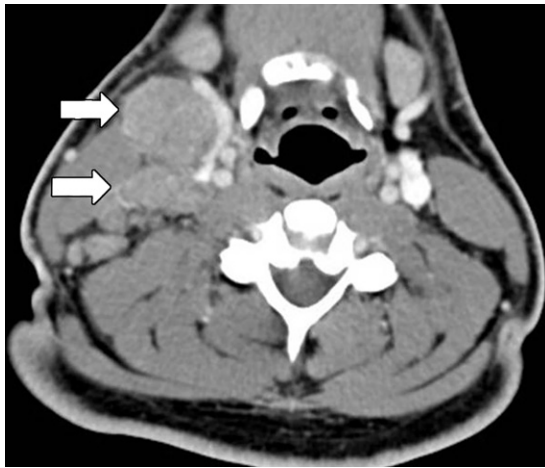


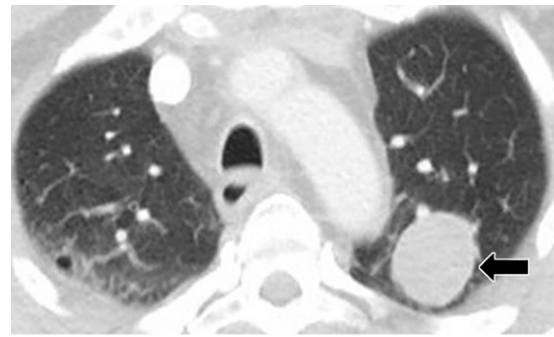
Figure 24. Histiocytic sarcoma in the cervical lymph nodes in a 20-year-old man who presented with a neck lump. Axial contrast-enhanced CT image of the neck shows enlarged cervical lymph nodes (arrows) on the right. The results of a biopsy confirmed histiocytic sarcoma, which was CD163 and CD68 positive. The patient underwent chemotherapy but had a recurrence within a year, with widespread metastasis.

increasing need for improved imaging methods, especially in the area of treatment response evaluation and monitoring, where the radiologist can make substantial contributions.

Disclosures of Conflicts of Interest.—**M.N.** *Activities related to the present article:* disclosed no relevant relationships. *Activities not related to the present article:* consultancy fees from WorldCare Clinical, Toshiba Medical Systems, and Daiichi Sankyo; grants from Merck, Toshiba Medical Systems, and AstraZeneca; and honoraria for lectures from Bayer and Roche. **Other activities:** disclosed no relevant relationships. **J.L.H.** *Activities related to the present article:* disclosed no relevant relationships. *Activities not related to the present article:* consultancy fees from Epizyme and Eli Lilly and royalties from Elsevier, Demos Medical, and Wolters Kluwer. **Other activities:** disclosed no relevant relationships.

References

- Emile JF, Ablu O, Fraitag S, et al. Revised classification of histiocytoses and neoplasms of the macrophage-dendritic cell lineages. *Blood* 2016;127(22):2672–2681.
- Haroche J, Cohen-Aubart F, Rollins BJ, et al. Histiocytoses: emerging neoplasia behind inflammation. *Lancet Oncol* 2017;18(2):e113–e125.
- Berres ML, Merad M, Allen CE. Progress in understanding the pathogenesis of Langerhans cell histiocytosis: back to histiocytosis X? *Br J Haematol* 2015;169(1):3–13.
- Lichtenstein L. Histiocytosis X: integration of eosinophilic granuloma of bone, Letterer-Siwe disease, and Schüller-Christian disease as related manifestations of a single nosologic entity. *AMA Arch Pathol* 1953;56(1):84–102.
- Nezelof C, Basset F, Rousseau MF. Histiocytosis X histogenetic arguments for a Langerhans cell origin. *Biomedicine (Paris)* 1973;18(5):365–371.
- Writing Group of the Histiocyte Society. Histiocytosis syndromes in children. *Lancet* 1987;1(8526):208–209.
- Badalian-Very G, Vergilio JA, Degar BA, et al. Recurrent BRAF mutations in Langerhans cell histiocytosis. *Blood* 2010;116(11):1919–1923.
- Nelson DS, Quispel W, Badalian-Very G, et al. Somatic activating ARAF mutations in Langerhans cell histiocytosis. *Blood* 2014;123(20):3152–3155.
- Zeng K, Ohshima K, Liu Y, et al. BRAFV600E and MAP2K1 mutations in Langerhans cell histiocytosis occur predominantly in children. *Hematol Oncol* 2017;35(4): 845–851.



a.



b.

Figure 25. Histiocytic sarcoma in the lung and adrenal gland in a 54-year-old man with abdominal discomfort. (a) Axial nonenhanced CT image of the chest shows a well-demarcated mass (arrow) in the left upper lobe. (b) Axial nonenhanced CT image of the abdomen shows a mass (arrow) in the right adrenal gland. The results of a lung biopsy were initially suspicious for lung cancer. However, the results from a specimen obtained during surgical resection confirmed CD163- and CD68-positive histiocytic sarcoma in the lung. The patient underwent chemotherapy. The adrenal lesion was subsequently resected, and biopsy results also confirmed histiocytic sarcoma.

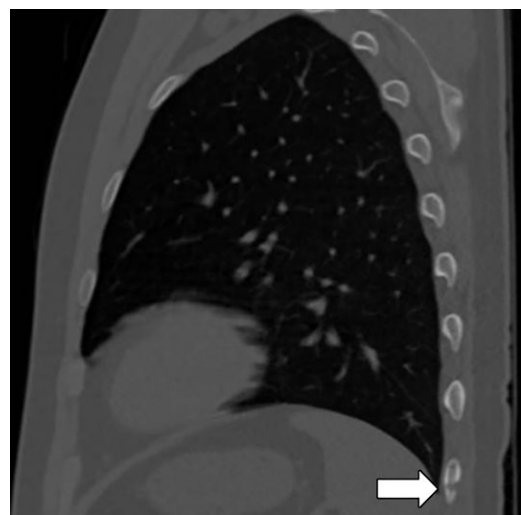


Figure 26. Interdigitating dendritic cell tumor in a 23-year-old man with chest wall pain. Sagittal CT image of the chest (bone window) shows a small lytic lesion (arrow) in the left 10th rib with cortical breakthrough. The lesion was resected, and the results of histological examination confirmed an atypical histiocytic neoplasm, a finding consistent with interdigitating dendritic cell tumor.

10. Héritier S, Emile JF, Barkaoui MA, et al. BRAF mutation correlates with high-risk Langerhans cell histiocytosis and increased resistance to first-line therapy. *J Clin Oncol* 2016;34(25):3023–3030.
11. Alayed K, Medeiros LJ, Patel KP, et al. BRAF and MAP2K1 mutations in Langerhans cell histiocytosis: a study of 50 cases. *Hum Pathol* 2016;52:61–67.
12. Selway JL, Harikumar PE, Chu A, Langlands K. Genetic homogeneity of adult Langerhans cell histiocytosis lesions: insights from BRAFV600E mutations in adult populations. *Oncol Lett* 2017;14(4):4449–4454.
13. Chakraborty R, Hampton OA, Shen X, et al. Mutually exclusive recurrent somatic mutations in MAP2K1 and BRAF support a central role for ERK activation in LCH pathogenesis. *Blood* 2014;124(19):3007–3015.
14. Chakraborty R, Burke TM, Hampton OA, et al. Alternative genetic mechanisms of BRAF activation in Langerhans cell histiocytosis. *Blood* 2016;128(21):2533–2537.
15. Haroche J, Charlotte F, Arnaud L, et al. High prevalence of BRAF V600E mutations in Erdheim-Chester disease but not in other non-Langerhans cell histiocytoses. *Blood* 2012;120(13):2700–2703.
16. Hutter C, Minkov M. Insights into the pathogenesis of Langerhans cell histiocytosis: the development of targeted therapies. *ImmunoTargets Ther* 2016;5:81–91.
17. Durham BH, Diamond EL, Abdel-Wahab O. Histiocytic neoplasms in the era of personalized genomic medicine. *Curr Opin Hematol* 2016;23(4):416–425.
18. Abila O, Weitzman S. Treatment of Langerhans cell histiocytosis: role of BRAF/MAPK inhibition. *Hematology Am Soc Hematol Educ Program* 2015;2015:565–570.
19. Rollins BJ. Genomic alterations in Langerhans cell histiocytosis. *Hematol Oncol Clin North Am* 2015;29(5):839–851.
20. Cantwell-Dorris ER, O’Leary JJ, Sheils OM. BRAFV600E: implications for carcinogenesis and molecular therapy. *Mol Cancer Ther* 2011;10(3):385–394.
21. Ascierto PA, Kirkwood JM, Grob JJ, et al. The role of BRAF V600 mutation in melanoma. *J Transl Med* 2012;10(1):85.
22. Tiacci E, Pettrossi V, Schiavoni G, Falini B. Genomics of hairy cell leukemia. *J Clin Oncol* 2017;35(9):1002–1010.
23. Barras D. BRAF mutation in colorectal cancer: an update. *Biomark Cancer* 2015;7(suppl 1):9–12.
24. Bösmüller H, Fischer A, Pham DL, et al. Detection of the BRAF V600E mutation in serous ovarian tumors: a comparative analysis of immunohistochemistry with a mutation-specific monoclonal antibody and allele-specific PCR. *Hum Pathol* 2013;44(3):329–335.
25. Cohn AL, Day BM, Abhyankar S, McKenna E, Riehl T, Puzanov I. BRAFV600 mutations in solid tumors, other than metastatic melanoma and papillary thyroid cancer, or multiple myeloma: a screening study. *OncoTargets Ther* 2017;10:965–971.
26. Nguyen-Ngoc T, Bouchaab H, Adjei AA, Peters S. BRAF alterations as therapeutic targets in non-small-cell lung cancer. *J Thorac Oncol* 2015;10(10):1396–1403.
27. Berres ML, Lim KP, Peters T, et al. BRAF-V600E expression in precursor versus differentiated dendritic cells defines clinically distinct LCH risk groups. *J Exp Med* 2014;211(4):669–683 [Published correction appears in *J Exp Med* 2015;212(2):281.].
28. Blombery P, Wong SQ, Lade S, Prince HM. Erdheim-Chester disease harboring the BRAF V600E mutation. *J Clin Oncol* 2012;30(32):e331–e332.
29. Haroun F, Millado K, Tabbara I. Erdheim-Chester disease: comprehensive review of molecular profiling and therapeutic advances. *Anticancer Res* 2017;37(6):2777–2783.
30. Haroche J, Cohen-Aubart F, Emile JF, et al. Dramatic efficacy of vemurafenib in both multisystemic and refractory Erdheim-Chester disease and Langerhans cell histiocytosis harboring the BRAF V600E mutation. *Blood* 2013;121(9):1495–1500.
31. Haroche J, Cohen-Aubart F, Emile JF, et al. Reproducible and sustained efficacy of targeted therapy with vemurafenib in patients with BRAF(V600E)-mutated Erdheim-Chester disease. *J Clin Oncol* 2015;33(5):411–418.
32. Diamond EL, Subbiah V, Lockhart AC, et al. Vemurafenib for BRAF V600-mutant Erdheim-Chester disease and Langerhans cell histiocytosis: analysis of data from the histology-independent, phase 2, open-label VE-BASKET Study. *JAMA Oncol* 2018;4(3):384–388.
33. Oneal PA, Kwitkowski V, Luo L, et al. FDA approval summary: vemurafenib for the treatment of patients with Erdheim-Chester Disease with the BRAFV600 mutation. *Oncologist*. 2018 Aug 17. [Epub ahead of print.]
34. Nishino M, Jagannathan JP, Krajewski KM, et al. Personalized tumor response assessment in the era of molecular medicine: cancer-specific and therapy-specific response criteria to complement pitfalls of RECIST. *AJR Am J Roentgenol* 2012;198(4):737–745.
35. Nishino M, Hatabu H, Johnson BE, McLoud TC. State of the art: response assessment in lung cancer in the era of genomic medicine. *Radiology* 2014;271(1):6–27.
36. Minkov M, Grois N, McClain K, et al. Langerhans cell histiocytosis: Histiocyte Society evaluation and treatment guidelines. Pitman, NJ: Histiocyte Society, 2009.
37. Pierro J, Vaiselbuh SR. Adult Langerhans cell histiocytosis as a diagnostic pitfall. *J Clin Oncol* 2016;34(6): e41–e45.
38. Girschikofsky M, Arico M, Castillo D, et al. Management of adult patients with Langerhans cell histiocytosis: recommendations from an expert panel on behalf of Euro-Histio-Net. *Orphanet J Rare Dis* 2013;8(1):72.
39. Yadav SP, Kharya G, Mohan N, et al. Langerhans cell histiocytosis with digestive tract involvement. *Pediatr Blood Cancer* 2010;55(4):748–753.
40. Ramzan M, Yadav SP. Langerhans cell histiocytosis presenting as isolated mediastinal mass in an infant. *Indian Pediatr* 2014;51(5):397–398.
41. Podjasek JO, Loftus CG, Smyrk TC, Wieland CN. Adult-onset systemic Langerhans cell histiocytosis mimicking inflammatory bowel disease: the value of skin biopsy and review of cases of Langerhans cell histiocytosis with cutaneous involvement seen at the Mayo Clinic. *Int J Dermatol* 2014;53(3):305–311.
42. Numakura S, Morikawa T, Ushiku T, Toyoshima T, Fukayama M. Langerhans cell histiocytosis of the urinary bladder in a patient with bladder cancer previously treated with intravesical Bacillus Calmette-Guérin therapy. *Pathol Res Pract* 2014;210(2):123–126.
43. Karimzada MM, Matthews MN, French SW, DeUgarte D, Kim DY. Langerhans cell histiocytosis masquerading as acute appendicitis: case report and review. *World J Gastrointest Endosc* 2017;9(3):139–144.
44. Yang S, Chen X, Zhang J, Fang Q. Isolated Langerhans cell histiocytosis of the sublingual gland in an adult. *Int J Clin Exp Pathol* 2015;8(10):13647–13650.
45. Gadner H, Grois N, Pötschger U, et al. Improved outcome in multisystem Langerhans cell histiocytosis is associated with therapy intensification. *Blood* 2008;111(5): 2556–2562.
46. Zaveri J, La Q, Yarmish G, Neuman J. More than just Langerhans cell histiocytosis: a radiologic review of histiocytic disorders. *RadioGraphics* 2014;34(7):2008–2024.
47. Meyer JS, Harty MP, Mahboubi S, et al. Langerhans cell histiocytosis: presentation and evolution of radiologic findings with clinical correlation. *RadioGraphics* 1995;15(5):1135–1146.
48. Stull MA, Kransdorf MJ, Devaney KO. Langerhans cell histiocytosis of bone. *RadioGraphics* 1992;12(4):801–823.
49. Aricò M, Girschikofsky M, Génereau T, et al. Langerhans cell histiocytosis in adults: report from the International Registry of the Histiocyte Society. *Eur J Cancer* 2003;39(16):2341–2348.
50. Nishino M, Itoh H, Hatabu H. A practical approach to high-resolution CT of diffuse lung disease. *Eur J Radiol* 2014;83(1):6–19.
51. Lacronique J, Roth C, Battesti JP, Basset F, Chretien J. Chest radiological features of pulmonary histiocytosis X: a report based on 50 adult cases. *Thorax* 1982;37(2):104–109.
52. Vassallo R, Ryu JH, Schroeder DR, Decker PA, Limper AH. Clinical outcomes of pulmonary Langerhans’ cell histiocytosis in adults. *N Engl J Med* 2002;346(7): 484–490.
53. Tazi A, Marc K, Dominique S, et al. Serial computed tomography and lung function testing in pulmonary Langerhans’ cell histiocytosis. *Eur Respir J* 2012;40(4):905–912.
54. Hidalgo A, Franquet T, Giménez A, Bordes R, Pineda R, Madrid M. Smoking-related interstitial lung diseases: radiologic-pathologic correlation. *Eur Radiol* 2006;16(11):2463–2470.
55. Prayer D, Grois N, Prosch H, Gadner H, Barkovich AJ. MR imaging presentation of intracranial disease associated with Langerhans cell histiocytosis. *AJNR Am J Neuroradiol* 2004;25(5):880–891.

56. Makras P, Samara C, Antoniou M, et al. Evolving radiological features of hypothalamo-pituitary lesions in adult patients with Langerhans cell histiocytosis (LCH). *Neuroradiology* 2006;48(1):37–44.
57. Martin-Duverneuil N, Idbaih A, Hoang-Xuan K, et al. MRI features of neurodegenerative Langerhans cell histiocytosis. *Eur Radiol* 2006;16(9):2074–2082.
58. Kilpatrick SE, Wenger DE, Gilchrist GS, Shives TC, Wollan PC, Unni KK. Langerhans' cell histiocytosis (histiocytosis X) of bone: a clinicopathologic analysis of 263 pediatric and adult cases. *Cancer* 1995;76(12):2471–2484.
59. Monsereenusorn C, Rodriguez-Galindo C. Clinical characteristics and treatment of Langerhans cell histiocytosis. *Hematol Oncol Clin North Am* 2015;29(5):853–873.
60. Samet J, Weinstein J, Fayad LM. MRI and clinical features of Langerhans cell histiocytosis (LCH) in the pelvis and extremities: can LCH really look like anything? *Skeletal Radiol* 2016;45(5):607–613.
61. Phillips M, Allen C, Gerson P, McClain K. Comparison of FDG-PET scans to conventional radiography and bone scans in management of Langerhans cell histiocytosis. *Pediatr Blood Cancer* 2009;52(1):97–101.
62. Yi X, Han T, Zai H, Long X, Wang X, Li W. Liver involvement of Langerhans' cell histiocytosis in children. *Int J Clin Exp Med* 2015;8(5):7098–7106.
63. Edelweiss M, Medeiros LJ, Suster S, Moran CA. Lymph node involvement by Langerhans cell histiocytosis: a clinicopathologic and immunohistochemical study of 20 cases. *Hum Pathol* 2007;38(10):1463–1469.
64. Chester W. Über Lipoidgranulomatose. *Virchows Arch Pathol Anat Physiol Klin Med* 1930;279(2):561–602.
65. Martineau P, Pelletier-Galarneau M, Zeng W. The imaging findings of Erdheim-Chester disease: a multimodality approach to diagnosis and staging. *World J Nucl Med* 2017;16(1):71–74.
66. Dion E, Graef C, Miquel A, et al. Bone involvement in Erdheim-Chester disease: imaging findings including periostitis and partial epiphyseal involvement. *Radiology* 2006;238(2):632–639.
67. Antunes C, Graça B, Donato P. Thoracic, abdominal and musculoskeletal involvement in Erdheim-Chester disease: CT, MR and PET imaging findings. *Insights Imaging* 2014;5(4):473–482.
68. Sedrak P, Ketonen L, Hou P, et al. Erdheim-Chester disease of the central nervous system: new manifestations of a rare disease. *AJNR Am J Neuroradiol* 2011;32(11):2126–2131.
69. Merritt H, Pfeiffer ML, Richani K, Phillips ME. Erdheim-Chester disease with orbital involvement: case report and ophthalmic literature review. *Orbit* 2016;35(4):221–226.
70. Young JR, Johnson GB, Murphy RC, Go RS, Broski SM. 18F-FDG PET/CT in Erdheim-Chester disease: imaging findings and potential BRAF mutation biomarker. *J Nucl Med* 2018;59(5):774–779.
71. Ponsiglione A, Puglia M, Barbuto L, et al. Cardiac involvement in Erdheim-Chester disease: MRI findings and literature revision. *Acta Radiol Open* 2015;4(9):2058460115592273.
72. Haroche J, Cluzel P, Toledano D, et al. Images in cardiovascular medicine: cardiac involvement in Erdheim-Chester disease—magnetic resonance and computed tomographic scan imaging in a monocentric series of 37 patients. *Circulation* 2009;119(25):e597–e598.
73. Brun AL, Touitou-Gottenberg D, Haroche J, et al. Erdheim-Chester disease: CT findings of thoracic involvement. *Eur Radiol* 2010;20(11):2579–2587.
74. Nikpanah M, Kim L, Mirmomen SM, et al. Abdominal involvement in Erdheim-Chester disease (ECD): MRI and CT imaging findings and their association with BRAFV600E mutation. *Eur Radiol* 2018 Mar 19. [Epub ahead of print.]
75. Destombes P. Adenitis with lipid excess, in children or young adults, seen in the Antilles or Mali: 4 cases. *Bull Soc Pathol Exot Filiales* 1965;58(6):1169–1175.
76. Rosai J, Dorfman RF. Sinus histiocytosis with massive lymphadenopathy: a newly recognized benign clinicopathological entity. *Arch Pathol* 1969;87(1):63–70.
77. Grabczynska SA, Toh CT, Francis N, Costello C, Bunker CB. Rosai-Dorfman disease complicated by autoimmune haemolytic anaemia: case report and review of a multisystem disease with cutaneous infiltrates. *Br J Dermatol* 2001;145(2):323–326.
78. Fernandez-Vega I, Santos-Juanes J, Ramsay A. Cutaneous Rosai-Dorfman disease following a classical Hodgkin lymphoma, nodular sclerosis subtype. *Am J Dermatopathol* 2014;36(3):280–281.
79. La Barge DV 3rd, Salzman KL, Harnsberger HR, et al. Sinus histiocytosis with massive lymphadenopathy (Rosai-Dorfman disease): imaging manifestations in the head and neck. *AJR Am J Roentgenol* 2008;191(6):W299–W306.
80. Sandoval-Sus JD, Sandoval-Leon AC, Chapman JR, et al. Rosai-Dorfman disease of the central nervous system: report of 6 cases and review of the literature. *Medicine (Baltimore)* 2014;93(3):165–175.
81. Mantilla JG, Goldberg-Stein S, Wang Y. Extranodal Rosai-Dorfman disease: clinicopathologic series of 10 patients with radiologic correlation and review of the literature. *Am J Clin Pathol* 2016;145(2):211–221.
82. Tian Y, Wang J, Ge J, Ma Z, Ge M. Intracranial Rosai-Dorfman disease mimicking multiple meningiomas in a child: a case report and review of the literature. *Childs Nerv Syst* 2015;31(2):317–323.
83. Karajgikar J, Grimaldi G, Friedman B, Hines J. Abdominal and pelvic manifestations of Rosai-Dorfman disease: a review of four cases. *Clin Imaging* 2016;40(6):1291–1295.
84. Cohen Aubart F, Haroche J, De Risi T, et al. La maladie de Rosai-Dorfman-Destombes est une histiocytose inflammatoire polymorphe: étude phénotypique multicentrique de 47 patients. *Rev Med Interne* 2015;36(suppl 1):A40–A41.
85. Jacobsen E, Shanmugam V, Jagannathan J. Rosai-Dorfman disease with activating KRAS mutation: response to cobimetinib. *N Engl J Med* 2017;377(24):2398–2399.
86. Shanmugam V, Margolskee E, Kluk M, Giorgadze T, Orazi A. Rosai-Dorfman disease harboring an activating KRAS K117N missense mutation. *Head Neck Pathol* 2016;10(3):394–399.
87. Fujiwara F, Hibi S, Imashuku S. Hypercytokinemia in hemophagocytic syndrome. *Am J Pediatr Hematol Oncol* 1993;15(1):92–98.
88. Fitzgerald NE, McClain KL. Imaging characteristics of hemophagocytic lymphohistiocytosis. *Pediatr Radiol* 2003;33(6):392–401.
89. Henter JI, Samuelsson-Horne A, Aricò M, et al. Treatment of hemophagocytic lymphohistiocytosis with HLH-94 immunochemotherapy and bone marrow transplantation. *Blood* 2002;100(7):2367–2373.
90. Zhu J, Su S, Zhou J, Li H. Interdigitating dendritic cell sarcoma presenting in the sigmoid colon mesentery: a case report and literature review. *Medicine (Baltimore)* 2017;96(16):e6210.